

Sodium Pancratistatin 3,4-*O*-Cyclic Phosphate, a Water-Soluble Synthetic Derivative of Pancratistatin, Is Highly Effective in a Human Colon Tumor Model[†]

Steven D. Shnyder,* Patricia A. Cooper, Nicola J. Millington, Jason H. Gill, and Michael C. Bibby

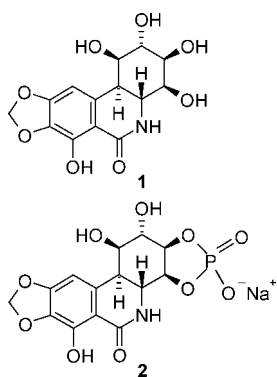
Institute of Cancer Therapeutics, University of Bradford, Richmond Road, Bradford, BD7 1DP, U.K.

Received September 7, 2007

Sodium pancratistatin 3,4-*O*-cyclic phosphate (**2**) is a novel water-soluble synthetic derivative of pancratistatin (**1**), a natural alkaloid constituent of Amaryllidaceae plants, that exhibits good cytostatic and antineoplastic activity but is highly insoluble. Unlike most other natural alkaloids it does not act by binding to tubulin, and its mechanism of action has yet to be fully elucidated. Here the efficacy of **2** in a human colon adenocarcinoma model, DLD-1, and some understanding of its mode of action are investigated. Agreeing with previous studies, low cytotoxicity *in vitro* was seen for **2** with IC₅₀'s of 253 and 19.7 μM for 1 and 96 h exposures, respectively. However *in vivo* the compound caused statistically significant tumor growth delays ($p < 0.01$) at its maximum tolerated dose, and significant vascular shutdown and tumor necrosis were observed. Like **1**, the compound appeared to have an unconventional mechanism of action with no effect on microtubule structure, yet causing a G₂/M block, while it was seen to disrupt mitochondrial function. The mechanism of action of **1** and **2** appears to be similar. Thus compound **2**, being considerably more soluble than **1**, has good potential as an anticancer agent, and further investigation is warranted.

The first reported isolation of the natural compound (+)-pancratistatin (**1**) was by Pettit and colleagues in 1984.^{1a} Pancratistatin is isolated from the tropical spider lily *Hymenocallis littoralis*, which is a member of the Amaryllidaceae family, and it has demonstrated promising anticancer activity *in vitro*. Due to initial problems with poor yields of **1**, poor solubility, and bioavailability, extensive further studies taking both horticultural^{1b,c} and synthetic^{1d-f} approaches led to investigations to make more soluble analogues. One of these studies led to the synthesis of sodium pancratistatin 3,4-*O*-cyclic phosphate (**2**).²

Unlike most other natural alkaloids, **1** does not act by binding to tubulin, and its mechanism of action has yet to be fully elucidated. Recent studies have suggested that **1** inhibits progression from G₀/G₁ to S-phase^{3a} and targets mitochondria in cancer cells *in vitro* to induce apoptosis.^{3b} On the basis of these findings, here we investigate the efficacy of **2** in a human colon adenocarcinoma cell line, DLD-1, and also gain some understanding of its action as an antitumor agent.



Results and Discussion

Compound **2** exhibited an almost 3-log improved solubility in aqueous solutions compared with **1**, with a solubility of at least 20 mgml⁻¹. This meant that it was possible to evaluate the compound

[†] Dedicated to Dr. G. Robert Pettit of Arizona State University for his pioneering work on bioactive natural products.

* To whom enquiries should be addressed. Tel: +44-1274-235898. Fax: +44-1274-233234. E-mail: S.D.Shnyder@Bradford.ac.uk.

Table 1. Significant *in Vivo* Activity of **2** Seen When Administered *i.v.* as a Single Dose

dose (mg kg ⁻¹)	mean RTV ₂ ^a (days)	max. % weight loss (day)
control	6.2	0.5
100	15.1 ^b	8.8

^a Mean tumor doubling time. ^b $p < 0.01$.

in vivo by the more clinically relevant intravenous route. Pancratistatin (**1**), due to its lack of solubility, could be formulated only to be applied intraperitoneally.

To confirm that DLD-1 would be a relevant model to select for screening **2** *in vivo*, we first evaluated its *in vitro* potency to compare it with previous studies.² The reason for wanting to use this line was due to the good vascularization observed when grown *in vivo* as subcutaneous xenograft tumors.^{4c} Compound **2** demonstrated relatively poor potency *in vitro*, with IC₅₀'s of 253 and 19.7 μM, respectively, for 1 and 96 h drug exposures versus the DLD-1 cell line. These figures are within a similar range to previous *in vitro* studies in a small panel of cancer cell lines² including the colon adenocarcinoma cell line KM20L2. This potency is approximately 100-fold less than reported for **1** and is probably due to the lack of endogenous nonspecific phosphatases, which are responsible for the cleavage to the active agent *in vivo*,^{4a} in the cell culture medium. The similarity of the screening results for **2**, combined with similarities in the cytotoxicities seen for DLD-1 and KM20L2 in the NCI 60-cell line screen of **1**,⁵ suggested that DLD-1 would be a suitable model to continue evaluation of **2** *in vivo*.

When the *in vivo* efficacy of **2** was evaluated, a statistically significant growth delay was seen when administered at maximum tolerated dose (MTD) compared to the control group (Table 1 and Figure 1). There was negligible toxicity, with the observed maximum weight loss well within the normal limits.

The extent of functional vascular elements (as determined by the incorporation of the Hoechst 33342 dye into the nuclei of functioning endothelial cells) was significantly affected by administration of **2** (Table 2) with all but the vasculature at the periphery of the DLD-1 tumor xenograft shut down 24 h after compound administration (Figure 2).

Histological evaluation of hematoxylin- and eosin-stained sections showed a significant increase in the amount of necrosis seen

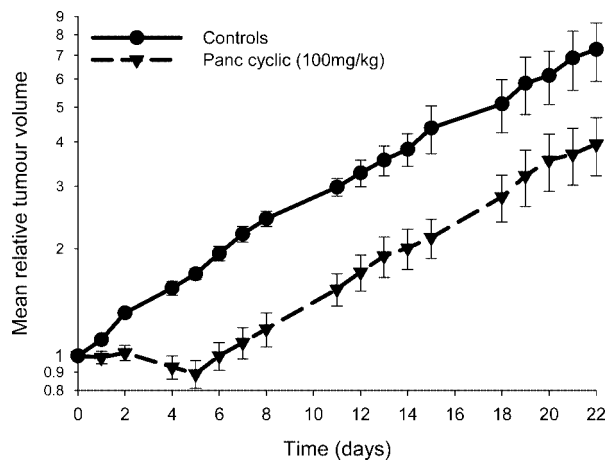


Figure 1. Efficacy of **2** administered at MTD as a single dose i.v. against s.c. implanted DLD-1 xenografts. Points represent mean \pm SD ($n = 8$).

Table 2. Significant Increase in Tumor Necrosis and Decrease in Functional Vasculature Seen 24 h after Administration of **2**

analysis	100 mg kg ⁻¹ of 2	control
% necrosis	95.3 ^a	8.1
% vasculature	0.6 ^a	6.5

^a $p < 0.01$.

after 24 h in DLD-1 tumors exposed to **2** (Table 2). Residual viable tissue was found mainly at the periphery of the tumor in a similar location to the functional vasculature, as described above (Figure 2).

In order to elucidate the mechanism of action for the significant vascular shutdown and necrosis observed, a few facets of the mechanism of action were evaluated. Disruption of microtubule structure is often linked with vascular damage,⁴ but immunocytochemical observation of microtubule structure in both **2**-treated DLD-1 and human umbilical vascular endothelial cells (HUVECs) showed no obvious disruption of the normal tubulin cytoskeletal structure (Figure 3a–i). Interestingly, although there was no obvious effect on microtubule structure, when **2** was administered at a dose

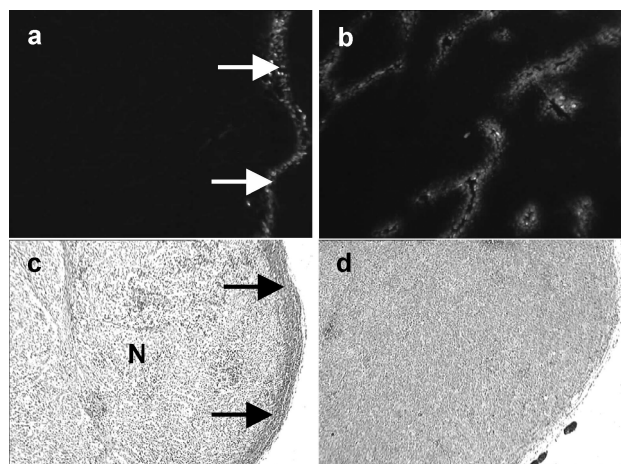


Figure 2. Images of Hoechst 33342-stained functional vascular elements in cryosections of DLD-1 tumor treated with **2** (a) 24 h after treatment compared with untreated tumor (b). Functional vasculature elements were seen only in the periphery of the tumor (arrows). Hematoxylin- and eosin-stained images of DLD-1 tumor treated with **2** from 24 h after treatment (c) compared with untreated tumor (d). Significant necrosis (N) seen centrally in the treated tumor, with viable tumor remaining at the periphery (arrows).

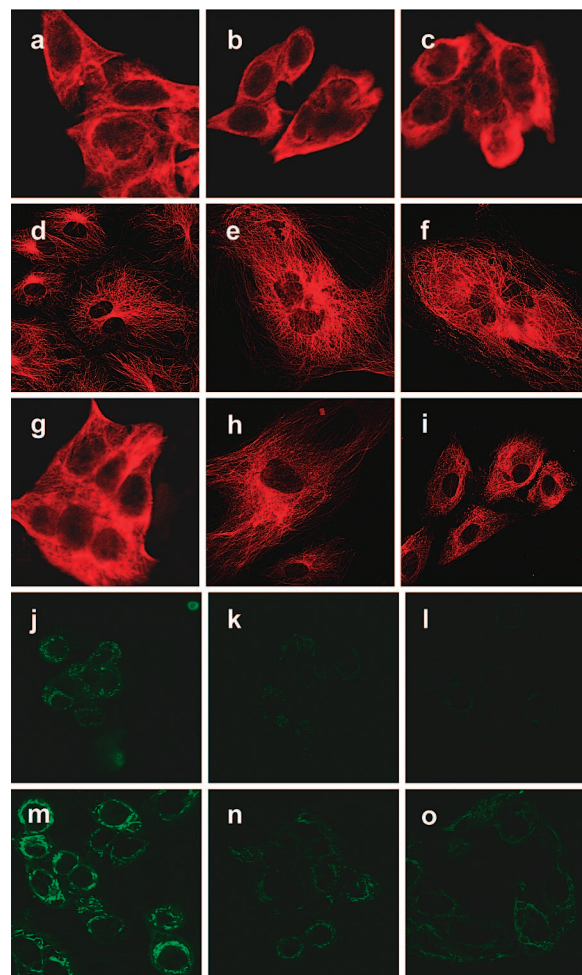


Figure 3. Compound **2** has no effect on microtubule structure but causes mitochondrial disruption. (a–c) DLD-1 cells and (d–f) HUVECs exposed to 250 μ M **2** for 1, 3, and 24 h, respectively, showing no disruption of normal microtubule structure similar to untreated DLD-1 cells (g) and HUVECs (h). Disruption is seen with the positive control compound paclitaxel at 440 nM (i). Progressive reduction of mitochondrial membrane potential with time as visualized by decrease in fluorescence of MitoTracker green FM solution is seen in DLD-1 cells treated with 250 μ M **2** at 4 (j), 7 (k), and 24 h (l) compared with untreated cultures imaged at the same times (m–o).

close to its IC₅₀, 250 μ M, cell cycle analysis demonstrated considerable accumulation of cells in G₂/M phase compared with the untreated control samples (Figure 4). However, unlike other agents where vascular targeting is part of their mechanism of action, such as for Auristatin PYE,^{4c} G₂/M arrest was not seen at subactive concentrations of 25 μ M. These results appear to conflict with previous findings for **1**^{3a} where arrest was seen at G₀/G₁ as opposed to the G₂/M arrest seen here (with the caveat that the earlier experiment was carried out with synchronized fibroblast populations as opposed to regularly growing colon adenocarcinoma cells).

It has previously been demonstrated that a loss of mitochondrial membrane potential, as denoted by a reduction in active uptake of a mitochondrion-selective probe, was observed over 24 h when tumor cells were treated with **1**.^{3b} Mitochondrial dysfunction leading to apoptosis has been linked to an increase in the amount of reactive oxygen species (ROS),⁶ and an increase in ROS following treatment with **1** has been reported,^{3b} thus suggesting that the mitochondria may be the site of action of this compound. Furthermore, perturbation of mitochondrial function has been reported as being key to vascular targeting for other agents.⁷ Thus after no evidence of tubulin disruption was seen as an explanation for the mechanism

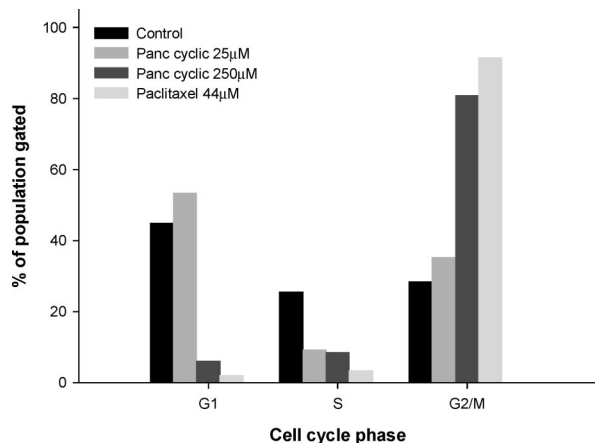


Figure 4. Cell cycle analyses of DLD-1 cells exposed to **2** showing a dose-related G₂/M stage block, with paclitaxel as a positive control compound.

of action of **2**, the mitochondrial membrane potential was evaluated in this study using a probe that accumulates in the mitochondria of actively respiring cells.⁸ As with the previous study on **1**,^{3b} it was seen that the fluorescent signal was greatly reduced over 24 h compared with the untreated control cells, thus suggesting that mitochondrial dysfunction has a role in the effects seen (Figure 3j–o).

Thus we have demonstrated here that the 3,4-*O*-cyclic phosphate salt of pancratistatin offers a way of progressing this promising molecule into the clinic by greatly improving solubility without loss of its antitumor activity. Further *in vivo* studies are warranted to evaluate the pharmacokinetic profile and to optimize the dose schedule of this compound.

Experimental Section

General Experimental Procedures. Compound **2** was synthesized as previously described² and provided by Professor G. R. Pettit, Cancer Research Institute, University of Arizona (Tempe, AZ). Compound **2** was dissolved to the appropriate concentration using sterile physiological saline for *in vivo* studies and cell culture medium for *in vitro* studies. For *in vivo* studies compounds were administered as single doses injected intravenously at 0.1 mL injection volume per 10 g of body weight. Paclitaxel (Sigma) was initially dissolved in DMSO and then diluted to the appropriate concentration using cell culture medium.

Animals. Female CD1-Foxn1tm immunodeficient nude mice (Charles River Laboratories, Margate, UK) age 6–8 weeks were used. Mice received CRM diet (SDS, Witham, UK) and water *ad libitum*. Mice were kept in cages in an air-conditioned room with regular alternating cycles of light and darkness. All animal procedures were carried out under a project license issued by the UK Home Office, and UKCCCR guidelines⁹ were followed throughout.

Cell Lines. The DLD-1 human colon adenocarcinoma cell line (from LGC Promochem, Middlesex, UK) was cultured in RPMI 1640 cell culture medium supplemented with 1 mM sodium pyruvate, 2 mM L-glutamine, and 10% fetal bovine serum (all from Sigma). Human umbilical cord endothelial cells (HUVECs) were isolated from umbilical cords from elective Caesarean sections performed at Bradford Royal Infirmary's Maternity Unit¹⁰ and cultured on 0.2% gelatin-coated tissue culture vessels in medium M199 supplemented with 100 mM sodium pyruvate, 200 mM L-glutamine, 5000 IU mL⁻¹ penicillin, 5 mg mL⁻¹ streptomycin (all from Sigma), and 10% human serum.^{4b}

Growth Inhibition Assays. Tumor cell growth inhibition was assessed using the MTT assay.¹¹ DLD-1 cells (1×10^4) were inoculated into each well of a 96-well plate and incubated overnight at 37 °C in a humidified atmosphere containing 5% CO₂. Compounds were diluted in complete cell culture medium to give a broad range of concentrations. Medium was removed from each well and replaced with compound or control solutions, and the plates then incubated for a further 1 or 96 h. For the 1 h plates, compound was removed after 1 h and fresh culture medium added for the remaining 95 h. After 96 h culture medium was

removed and 200 µL of 0.5 mg mL⁻¹ MTT solution (Sigma) in complete medium added to each well. Following a further 4 h incubation, the solution was removed from each well and 150 µL of DMSO (Sigma) added to solubilize the formazan crystals resulting from MTT conversion. Absorbance values for the resulting solutions were read at 550 nm on a microplate reader, and cell survival was calculated as the absorbance of treated cells divided by the control. Results were expressed in terms of IC₅₀ values (i.e., concentration of compound required to kill 50% of cells), and all experiments were performed in triplicate.

Immunocytochemical Analysis of Microtubule Disruption. DLD-1 cells (5000) were seeded into each well of a Nunc eight-well chambered cover glass (Fisher Scientific, Loughborough, UK), or for analysis with HUVECs, 75 000 cells were seeded onto 2% gelatin-coated sterilized glass cover slips in six-well plates. In both cases cells were left to adhere for 24 h under normal incubation conditions. Compound **2**, at a range of concentrations, was then added to each culture for varying incubation times. The medium was then removed and fresh medium added for a further incubation of 1 h. Paclitaxel was administered as a positive control compound. Medium was then removed, and the cells were fixed in precooled methanol at –20 °C for 30 min. After two washes in PBS (all incubations at room temperature from this stage), cells were incubated in the primary monoclonal antibody mouse anti-α-tubulin (Sigma) at a dilution of 1:500 in PBS for 30 min. After three further washes in PBS, the secondary antibody, TRITC-conjugated rabbit antimouse IgG (Dako, Ely, UK), was added at a dilution of 1:50 for 30 min. After three final washes, the cultures were mounted in Vectashield (Vector Laboratories, Peterborough, UK) and stored at 4 °C until analysis. Cells were analyzed and images captured with a Zeiss LSM510 confocal system attached to an Axiovert 200 M inverted microscope using LSM510 software (all from Zeiss, Welwyn Garden City, UK).

Cell Cycle Analysis. DLD-1 cells in exponential growth were treated with a range of concentrations of **2** or paclitaxel as a positive control for G₂/M cell cycle block for 6 h. Following further incubation in drug-free medium for 24 h, cells were processed for analysis to check progression through the cell cycle using a method based on those of Ormerod.¹² A cell cycle profile was then obtained with a Becton Dickinson flow cytometer (Oxford, UK).

Evaluation of Mitochondrial Damage. Each well of a Nunc eight-well chambered cover glass was seeded with 5000 DLD-1 cells and either left untreated or treated with 250 µM compound **2** for 4, 7, or 24 h. Following incubation and washing, cells were incubated with 100 nM MitoTracker Green FM solution (Invitrogen, Paisley, UK) for 15 min. Uptake of MitoTracker solution into cells was analyzed, and images were captured with the confocal system as described above.

Tumor System. Tumors were excised from a donor animal, placed in sterile physiological saline containing antibiotics, and cut into small fragments of approximately 2 mm³. Under brief general inhalation anesthesia, DLD-1 tumor fragments were implanted in the left flank of each mouse using a trocar. Once the tumors could accurately be measured by callipers (mean tumor volume of 32 mm³), the mice were allocated into groups of eight by restricted randomization to keep the group mean tumor size variation to a minimum.

Chemotherapy Studies. Compound **2** was administered by a single intravenous injection, with the day of therapy designated day 0. The maximum tolerated dose (MTD) of **2** was established in the CD1-Foxn1tm model at 100 mg kg⁻¹, and efficacy was assessed as previously described^{13a}. Briefly, daily two-dimensional caliper measurements of the tumors were taken, with volumes calculated using the formula (a^2b)/2, where a is the smaller and b the larger tumor diameter. Tumor volume was then normalized to the respective volume on day 0, and semilog plots of relative tumor volume (RTV) versus time were made. Mann–Whitney U tests were performed to determine the statistical significance of any differences in growth rate (based on tumor volume doubling time) between control and treated groups.

Assessment of Vascular Shutdown and Tumor Necrosis. In order to further investigate the mechanism of action of **2** *in vivo*, the effects of treatment on the functional vasculature and development of necrosis in DLD-1 tumors were assessed as previously described.^{13a} Tumors were set up in both flanks of six mice, and treatment with **2** at MTD was carried out once the tumors had reached a minimum diameter of 7 mm to ensure that an established tumor vasculature was in place. At 24 h after treatment three mice were taken for assessment, with the final three mice serving as a control group. Hoechst 33342 (bisBenz-

imide, Sigma, Poole, UK) was used to assess the functional tumor vasculature.^{13b,3b} Hoechst 33342 was dissolved in sterile saline and injected intravenously by the tail vein at 40 mg kg⁻¹. One minute after injection the mice were euthanised by cervical dislocation and the tumors carefully and rapidly excised. One tumor from each mouse was then wrapped in aluminum foil and immediately immersed in liquid nitrogen and stored at -80 °C until ready for ultracryotomy, while the other tumor was immersion fixed in 10% neutral buffered formalin for 24 h and processed for paraffin embedding.

Frozen sections of 10 μm thickness were taken at approximately 100 μm intervals through the tumor. Five random fields from each of five random sections were examined for each tumor under UV illumination using a Leica DMRB microscope, with images captured digitally through a JVC 3-CCD camera and processed using AcQuis (Synoptics, Cambridge, UK) software. Functional vasculature was assessed by placing a cm² grid over the captured digital image and counting the number of points on the grid that overlay fluorescently stained cells. Comparisons were made between percentage vasculature in control and treated tumors. For each animal 5 μm thick paraffin sections were taken and stained with hematoxylin and eosin to assess hemorrhagic necrosis. Digital images were captured using the same system as above but with bright-field illumination. Student *t*-tests were performed to determine the statistical significance of any differences between control and treated groups.

Acknowledgment. We would like to thank B. Cronin for her technical assistance. This work has been supported by Cancer Research UK Programme Grant C7589/A5953 (S.D.S., P.A.C., N.J.M., J.H.G., M.C.B.) and Cancer Research UK Professorial Support Grant C7589/A5954 (M.C.B.).

References and Notes

- (1) (a) Pettit, G. R.; Gaddamidi, V.; Cragg, G. M. *J. Nat. Prod.* **1984**, *47*, 1018–1020. (b) Pettit, G. R.; Gaddamidi, V.; Herald, D. L.; Singh, S. B.; Cragg, G. M.; Schmidt, J. M.; Boettner, F. E.; Williams, M.; Sagawa, Y. *J. Nat. Prod.* **1986**, *49*, 995–1002. (c) Pettit, G. R.; Pettit, G. R.; Groszek, G.; Backhaus, R. A.; Doubek, D. L.; Barr, R. J.; Meerow, A. W. *J. Nat. Prod.* **1995**, *58*, 756–759. (d) Rinner, U.; Hillebrenner, H. L.; Adams, D. R.; Hudlicky, T.; Pettit, G. R. *Bioorg. Med. Chem. Lett.* **2004**, *14*, 2911–2915. (e) Pettit, G. R.; Melody, N.; Herald, D. L. *J. Org. Chem.* **2001**, *66*, 2583–2587. (f) Pettit, G. R.; Melody, N.; Herald, D. L.; Knight, J. C.; Chapuis, J. C. *J. Nat. Prod.* **2007**, *70*, 417–422.
- (2) Pettit, G. R.; Melody, N.; Herald, D. L. *J. Nat. Prod.* **2004**, *67*, 322–327.
- (3) (a) Mutsuga, M.; Kojima, K.; Yamashita, M.; Ohno, T.; Ogihara, Y.; Inoue, M. *Biol. Pharm. Bull.* **2002**, *25*, 223–228. (b) McLachlan, A.; Kekre, N.; McNulty, J.; Pandey, S. *Apoptosis* **2005**, *10*, 619–630.
- (4) (a) Dark, G. G.; Hill, S. A.; Prise, V. E.; Tozer, G. M.; Pettit, G. R.; Chaplin, D. J. *Cancer Res.* **1997**, *57*, 1829–1834. (b) Grosios, K.; Holwell, S. E.; McGown, A. T.; Pettit, G. R.; Bibby, M. C. *Br. J. Cancer* **1999**, *81*, 1318–1327. (c) Shnyder, S. D.; Cooper, P. A.; Millington, N. J.; Pettit, G. R.; Bibby, M. C. *Int. J. Oncol.* **2007**, *31*, 353–360.
- (5) NCI screening data for pancratistatin found at: <http://dtp.nci.nih.gov/dtpstandard/servlet/MeanGraphSummary?searchtype=namestartsandchemnameboolean=andandoutputformat=htmlandsearchlist=pancratistatinandSubmit=Submit>.
- (6) Fleury, C.; Mignotte, B.; Vayssiere, J. L. *Biochimie* **2002**, *84*, 131–141.
- (7) Don, A. S.; Kisker, O.; Dilda, P.; Donoghue, N.; Zhao, X.; Decollogne, S.; Creighton, B.; Flynn, E.; Folkman, J.; Hogg, P. J. *Cancer Cell* **2003**, *3*, 497–509.
- (8) Poot, M.; Zhang, Y. Z.; Kramer, J. A.; Wells, K. S.; Jones, L. J.; Hanzel, D. K.; Lugade, A. G.; Singer, V. L.; Haugland, R. P. *J. Histochem. Cytochem.* **1996**, *44*, 1363–1372.
- (9) Workman, P.; Twentyman, P.; Balkwill, F.; Balmain, A.; Chaplin, D.; Double, J.; Embleton, J.; Newell, D.; Raymond, R.; Stables, J.; Stephens, T.; Wallace, J. *Br. J. Cancer* **1998**, *77*, 1–10.
- (10) Jaffe, E. A.; Nachman, R. L.; Becker, C. G.; Minick, C. R. *J. Clin. Invest.* **1973**, *52*, 2745–2756.
- (11) Mosmann, T. *J. Immunol. Methods* **1983**, *65*, 55–63.
- (12) Ormerod, M. G. *Flow Cytometry: a Practical Approach*, 3rd. ed.; Oxford University Press: Oxford, United Kingdom, 2000.
- (13) (a) Shnyder, S. D.; Cooper, P. A.; Gyselinck, N.; Hill, B. T.; Double, J. A.; Bibby, M. C. *Anticancer Res.* **2003**, *23*, 4815–4820. (b) Quinn, P. K.; Bibby, M. C.; Cox, J. A.; Crawford, S. M. *Br. J. Cancer* **1992**, *66*, 323–330. (c) Smith, K. A.; Hill, S. A.; Begg, A. C.; Denekamp, J. *Br. J. Cancer* **1988**, *57*, 247–253.

NP070477P